J|A|C|S ARTICLES

Published on Web 05/11/2010

# Gas-Phase Vibrational Spectroscopy of Microhydrated Magnesium Nitrate Ions $[MgNO_3(H_2O)_{1-4}]^+$

Ling Jiang, Torsten Wende, Risshu Bergmann, Gerard Meijer, and Knut R. Asmis*

*Fritz-Haber-Institut der Max-Planck-Gesellschaft, Faradayweg 4-6, D-14195 Berlin, Germany*

Received February 9, 2010; E-mail: asmis@fhi-berlin.mpg.de

***Abstract:*** Infrared photodissociation spectra of buffer-gas-cooled $[MgNO_3(H_2O)_n]^+$ complexes with $n = 1-4$ are measured in the O−H stretching region. The observed bands are assigned to the excitation of the symmetric and antisymmetric stretching modes of the water molecules. The structural assignment of the spectra is aided by density functional theory calculations (B3LYP/6-311+G(d,p)) on energetically low-lying isomers, including the calculation of harmonic and anharmonic vibrational frequencies, as well as dissociation energies. The nitrate anion binds to the Mg dication in a bidentate fashion, occupying two coordination sites. The water molecules fill the remaining binding sites of the Mg cation, completing the first coordination shell at $n = 4$ and forming a stable six-fold-coordinated complex, the structure of which persists up to room temperature.

## 1. Introduction

Atmospheric aerosols have a significant impact on the Earth's climate because they increase the reflection of solar radiation.[1] Mineral dust and sea salts are among the most important aerosol sources, and magnesium is one of their most abundant components. These aerosols can be entrained in the air for weeks, have highly reactive surfaces, and thus react with pollutants such as nitrogen oxides to form nitrate salts. Consequently, magnesium nitrates are expected to play a crucial role in determining the properties of aged aerosols.[2,3]

Knowledge of how salts are solvated in aqueous media is of fundamental importance and helps, in particular, to understand the spectroscopic and chemical properties of aerosol particles. The long-standing view of the air−aqueous interface of inorganic salt solutions, i.e., that these interfaces are devoid of ions, has recently been corrected (see for example ref 4 and references therein). Ions with large polarizability, such as larger halide anions, have been shown to have a propensity for surface solvation.[4] Nitrate ions have also been predicted to prefer interfacial rather than bulk solvation.[5] Interestingly, for nitric acid solutions, acid dissociation is thermodynamically disfavored at the water−air interface, so nitrate ions are bulk-solvated and molecular $HNO_3$ is present at the surface.[6−8] The situation is different for salts, also because of the enhanced formation of ion pairs, and nitrate ions are present and cause perturbation of the interfacial water at the air−aqueous interface of mono-[9] and divalent[10] metal nitrate solutions. The formation of ion pairs at the interface critically depends on the salt concentration[11] as well as the size and charge of the metal ion.[12] In sufficiently dilute solutions (seven water molecules per nitrate at the interface), relatively free, dehydrated nitrate ions exist at the interface.[13]

Typical binding motifs found in hydrated salts can be characterized at the molecular level by a combination of gas-phase experiments and quantum chemical calculations on isolated clusters. Bare and partially hydrated (microhydrated) magnesium nitrate clusters serve as model systems for magnesium-nitrate-containing aerosols. Oomens et al. have studied the divalent metal nitrate anions $M(NO_3)_3^-$ and $M_2(NO_3)_5^-$, where M represents a group II metal dication, using infrared multiple photon dissociation (IRMPD) spectroscopy in the region of the nitrate stretches (900−1600 $cm^{-1}$),[14,15] showing that nitrate, in the absence of water, prefers to bind in a bidentate fashion to a six-fold-coordinated metal dication. Schröder and co-workers have studied $[MgNO_3(H_2O)_{1-7}]^+$ complexes using mass spectrometry and the $[MgNO_3(H_2O)_3]^+$ complex with IRMPD

(1) Ramanathan, V.; Crutzen, P. J.; Kiehl, J. T.; Rosenfeld, D. *Science* **2001**, *294*, 2119.
(2) Li, X. H.; Zhao, L. J.; Dong, J. L.; Xiao, H. S.; Zhang, Y. H. *J. Phys. Chem. B* **2008**, *112*, 5032.
(3) Gibson, E. R.; Hudson, P. K.; Grassian, V. H. *J. Phys. Chem. A* **2006**, *110*, 11785.
(4) Liu, D. F.; Ma, G.; Levering, L. M.; Allen, H. C. *J. Phys. Chem. B* **2004**, *108*, 2252.
(5) Salvador, P.; Curtis, J. E.; Tobias, D. J.; Jungwirth, P. *Phys. Chem. Chem. Phys.* **2003**, *5*, 3752.
(6) Kido Soule, M. C.; Blower, P. G.; Richmond, G. L. *J. Phys. Chem. A* **2007**, *111*, 3349.
(7) Dang, L. X.; Chang, T. M.; Roeselova, M.; Garrett, B. C.; Tobias, D. J. *J. Chem. Phys.* **2006**, 124.
(8) Bianco, R.; Wang, S. Z.; Hynes, J. T. *J. Phys. Chem. A* **2008**, *112*, 9467.
(9) Schnitzer, C.; Baldelli, S.; Shultz, M. J. *J. Phys. Chem. B* **2000**, *104*, 585.
(10) Xu, M.; Tang, C. Y.; Jubb, A. M.; Chen, X. K.; Allen, H. C. *J. Phys. Chem. C* **2009**, *113*, 2082.
(11) Zhang, Y. H.; Choi, M. Y.; Chan, C. K. *J. Phys. Chem. A* **2004**, *108*, 1712.
(12) Xu, M.; Larentzos, J. P.; Roshdy, M.; Criscenti, L. J.; Allen, H. C. *Phys. Chem. Chem. Phys.* **2008**, *10*, 4793.
(13) Xu, M.; Tang, C. Y.; Jubb, A. M.; Xiangke, C.; Allen, H. C. *J. Phys. Chem. C* **2009**, 2082.
(14) Leavitt, C. M.; Oomens, J.; Dain, R. P.; Steill, J.; Groenewold, G. S.; Van Stipdonk, M. J. *J. Am. Soc. Mass Spectrom.* **2009**, *20*, 772.
(15) Oomens, J.; Myers, L.; Dain, R.; Leavitt, C.; Pham, V.; Gresham, G.; Groenewold, G.; Van Stipdonk, M. *Int. J. Mass Spectrom.* **2008**, *273*, 24.



**10.1021/ja1011806** 

spectroscopy in the nitrate stretching region.[16] The latter confirmed the bidentate binding motif of the nitrate to the Mg dication. Microhydrated dications, e.g., $Ca^{2+}(H_2O)_n$,[17−19] have been shown to prefer internal solvation, with six water molecules comprising the first hydration shell. In contrast, microhydrated metal monocations as well as $NO_3^-$ do exhibit a pronounced tendency for the formation of intermolecular hydrogen bonds before the first hydration shell is complete.[20−23]

Several groups have performed computational studies on the structures of $[MgNO_3(H_2O)_n]^+$ complexes.[11,16,24] Schröder et al.[16] systematically studied microhydrated complexes with up to $n = 7$ at the MP2/aug-cc-pVDZ level of theory. They predicted that the Mg dication prefers six-fold coordination; i.e., it is fully coordinated at $n = 4$, with the nitrate occupying two binding sites (bidentate binding motif). The fifth water molecule then adds to the second hydration shell of the cation. Up to $n = 6$, bidentate coordination of the nitrate is the lowest in energy, but the tendency for monodentate coordination increases with increasing hydration. Solvent-shared and solvent-separated ion pairs were found to be considerably higher in energy (>0.5 eV), suggesting that significantly more water molecules need to be added to separate the two ions.

In the present study, we focus on a size-dependent characterization of the first coordination shell of a microhydrated Mg dication in the presence of a counterion (nitrate). First, the experimental setup is described. This includes an optical multipass cell, which allows increasing the photon fluence such that IRMPD spectra can be measured. Single-photon photodissociation of the $[MgNO_3(H_2O)He]^+$ complex is also measured to test the reliability of the multiple-photon dissociation setup. Temperature-dependent IRMPD spectra of $[MgNO_3(H_2O)_4]^+$ up to room temperature are measured to test its structural stability. The structural assignment of the spectra is aided by density functional calculations. The combination of experimental and simulated IR spectra allows for an unambiguous identification of the lowest-energy structures of microhydrated magnesium nitrate complexes.

## 2. Experimental Details

The experiments are carried out using an ion trap−tandem mass spectrometer system.[25,26] Briefly, gas-phase ions are continuously produced in a commercial Z-spray source from a $5 \times 10^{-3}$ M aqueous solution of magnesium nitrate. A beam of positive ions passes through a 4 mm diameter skimmer and is then collimated in a radiofrequency (rf) decapole ion guide. Parent ions are mass-selected in a quadrupole mass filter, deflected by 90° in an electrostatic quadrupole deflector, and focused into a gas-filled rf ring electrode ion trap. To allow for continuous ion loading and ion thermalization, the trap is continuously filled with He gas at an ion trap temperature of 12 K. After loading the trap for 98 ms, all ions are extracted from the ion trap and focused both temporally and spatially into the center of the extraction region of an orthogonally mounted linear time-of-flight (TOF) mass spectrometer. Here, they interact with the IR laser pulse from a Laservision OPO/OPA IR laser.[27] The table-top laser produces 7 ns/15 mJ pulses at 10 Hz with a spectral bandwidth of 2−3 $cm^{-1}$. The laser wavelength was calibrated using a photoacoustic cell filled with ammonia.

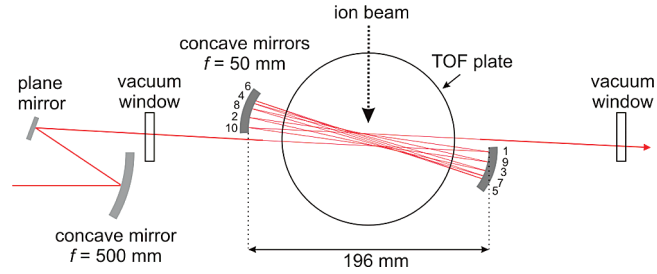


***Figure 1.*** Schematic of the multipass cell setup. The distance between the cell mirrors, which are installed inside the vacuum chamber adjacent to the extraction plates (dotted line) of the TOF mass spectrometer, determines the number of passes. Eleven passes are used for the present experiments.

To increase the fluence as well as the optical path length of the laser pulse through the ion cloud, a Herriott-type multipass cell[28−30] is installed inside the vacuum chamber encompassing the TOF extraction plates (see Figure 1). The multipass cell consists of two gold-coated spherical mirrors ($f = 50$ mm), separated by ∼20 cm to accommodate 10 reflections. It is installed off-axis (with respect to the line connecting the centers of the vacuum windows) such that the reflected laser beam exits the vacuum chamber on the side opposite that from which it entered, in order to allow monitoring of the pulse energy after the interaction zone. The IR laser beam is focused close to the center of the multipass cell by an external gold-coated spherical mirror ($f = 500$ mm).

## 3. Results

Experimental IRMPD spectra of $[MgNO_3(H_2O)_n]^+$, with $n = 1−4$, are shown in the bottom row of Figure 2, and band positions are listed in Table 1. The sum of the fragment ion yield is plotted as a function of the laser wavenumber. Under the present conditions, only loss of neutral water molecules is detected; i.e., the ionic $Mg^{2+}−NO_3^-$ bond stays intact. At higher pulse energies (∼7 mJ, measured directly after the OPA), all water-loss channels are observed, including the formation of bare $MgNO_3^+$ (loss of all water molecules). At lower pulse energies (∼2.3 mJ), mainly loss of a single water molecule is detected for $n > 1$.

The IRMPD spectrum for $n = 1$ shows three absorption features: an intense, narrower band at 3589 $cm^{-1}$; a less intense group of at least three peaks centered at 3637 $cm^{-1}$; and a weak absorption band at 3564 $cm^{-1}$. The two main bands at 3589 and 3637 $cm^{-1}$ are 68 and 119 $cm^{-1}$ red-shifted from the symmetric ($\nu_S$, 3657 $cm^{-1}$) and antisymmetric ($\nu_A$, 3756 $cm^{-1}$)

(16) Jagoda-Cwiklik, B.; Jungwirth, P.; Rulisek, L.; Milko, P.; Roithova, J.; Lemaire, J.; Maitre, P.; Ortega, J. M.; Schröder, D. *ChemPhysChem* **2007**, *8*, 1629.
(17) Bush, M. F.; O'Brien, J. T.; Prell, J. S.; Wu, C. C.; Saykally, R. J.; Williams, E. R. *J. Am. Chem. Soc.* **2009**, *131*, 13270.
(18) Bush, M. F.; Saykally, R. J.; Williams, E. R. *J. Am. Chem. Soc.* **2008**, *130*, 15482.
(19) Bush, M. F.; Saykally, R. J.; Williams, E. R. *ChemPhysChem* **2007**, *8*, 2245.
(20) Weinheimer, C. J.; Lisy, J. M. *J. Chem. Phys.* **1996**, *105*, 2938.
(21) Walker, N. R.; Walters, R. S.; Tsai, M.-K.; Jordan, K. D.; Duncan, M. A. *J. Phys. Chem. A* **2005**, *109*, 7057.
(22) Inokuchi, Y.; Ohshimo, K.; Misaizu, F.; Nishi, N. *J. Phys. Chem. A* **2004**, *108*, 5034.
(23) Goebbert, D. J.; Garand, E.; Wende, T.; Bergmann, R.; Meijer, G.; Asmis, K. R.; Neumark, D. M. *J. Phys. Chem. A* **2009**, *113*, 7584.
(24) Li, X. H.; Dong, J. L.; Xiao, H. S.; Lu, P. D.; Hu, Y. A.; Zhang, Y. H. *Sci. China Ser. B−Chem.* **2008**, *51*, 128.
(25) Goebbert, D. J.; Meijer, G.; Asmis, K. R. *AIP Conf. Proc.* **2009**, *1104*, 22.
(26) Goebbert, D. J.; Wende, T.; Bergmann, R.; Meijer, G.; Asmis, K. R. *J. Phys. Chem. A* **2009**, *113*, 5874.
(27) Bosenberg, W. R.; Guyer, D. R. *J. Opt. Soc. Am. B* **1993**, *10*, 1716.
(28) Herriott, D. R.; Schulte, H. J. *Appl. Opt.* **1965**, *4*, 883.
(29) Gross, M.; Hermann, G.; Scharmann, A. *Spectrochim. Acta B−At. Spectrosc.* **1989**, *44*, 597.
(30) Kaur, D.; Desouza, A. M.; Wanna, J.; Hammad, S. A.; Mercorelli, L.; Perry, D. S. *Appl. Opt.* **1990**, *29*, 119.

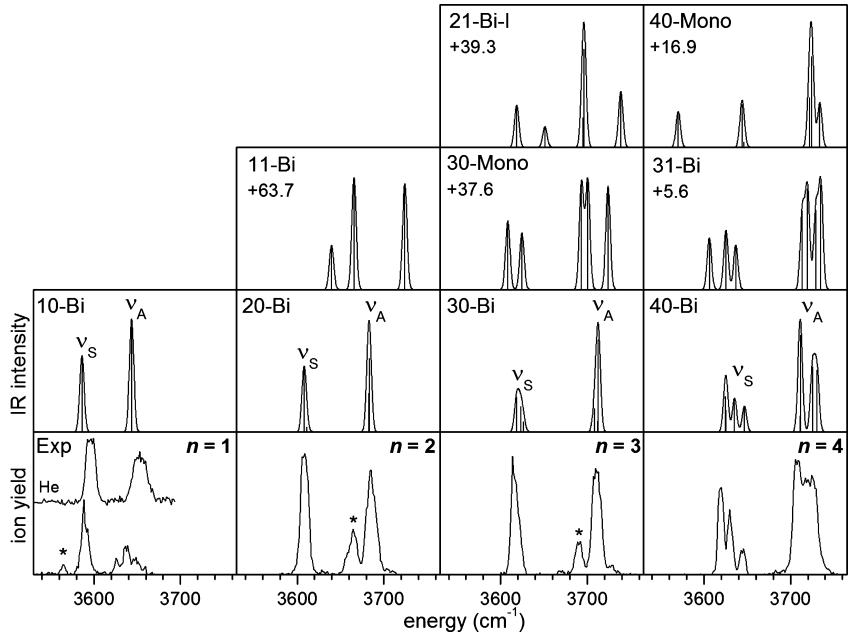


***Figure 2.*** Experimental IRMPD spectra (bottom row) and simulated linear IR spectra (upper rows) of $[MgNO_3(H_2O)_{1-4}]^+$ complexes. The IRPD spectrum of $[MgNO_3(H_2O)He]^+$ is also shown. Bands that are not assigned to an excitation of fundamental states are marked with an asterisk (see text). Simulated spectra, derived from harmonic frequencies and intensities (see Table 1), are shown for the B3LYP/6-311+G(d,p) global minimum energy structures (second row from bottom) and, when possible, also for other structural candidates (see Figure 4 for the corresponding geometric structures). Relative energies are given in kJ/mol.

***Table 1.*** Experimental IRMPD Band Positions (cm$^{-1}$), B3LYP/6-311G+(d,p) Vibrational Frequencies (cm$^{-1}$), and Intensities (km/mol) for $[MgNO_3(H_2O)_n]^+$ Complexes[a]

| *n* | exptl frequency | mode[b] | harmonic frequency[c] | scaled harmonic frequency | anharmonic frequency[d] |
|---|---|---|---|---|---|
| 1 | 3637 | $\nu_A$ | 3795 ($b_2$, 286) | 3628 | 3603 (7118) |
| | 3564 | | | | |
| | 3589 | $\nu_S$ | 3736 ($a_1$, 193) | 3571 | 3556 (7033) |
| 2 | 3685 | $\nu_A$ | 3837 (*a*, 311), 3836 (*b*, 164) | 3668, 3667 | 3651 (7251), 3653 (7257) |
| | 3665 | | | | |
| | 3608 | $\nu_S$ | 3761 (*a*, 20), 3758 (*b*, 268) | 3596, 3593 | 3591 (7136), 3588 (7130) |
| 3 | 3710 | $\nu_A$ | 3868 (*a*′, 434), 3866 (*a*″, 50), 3863 (*a*′, 110) | 3697, 3696, 3693 | 3671 (7293), 3670 (7285), 3671 (7240) |
| | 3692 | | | | |
| | 3614 | $\nu_S$ | 3777 (*a*′, 49), 3774 (*a*″, 122), 3769 (*a*′, 165) | 3611, 3608, 3604 | 3599 (7154), 3596 (7142), 3594 (7095) |
| 4 | 3724, 3717, 3706 | $\nu_A$ | 3886 (*a*″, 175), 3881 (*a*′, 183), 3866 (*a*′, 272), 3865 (*a*″, 46) | 3715, 3710, 3696, 3695 | 3693 (7297), 3691 (7280), 3677 (7303), 3684 (7318) |
| | 3646, 3630, 3620 | $\nu_S$ | 3799 (*a*″, 73), 3787 (*a*′, 95), 3777 (*a*′, 61), 3776 (*a*″, 100) | 3632, 3620, 3611, 3610 | 3622 (7164), 3607 (7123), 3607 (7168), 3606 (7165) |

[a] Harmonic, scaled harmonic (0.956), and anharmonic frequencies of the lowest-energy structure of $n = 1-4$ are listed. [b] Symmetric ($\nu_S$) and antisymmetric ($\nu_A$) O−H stretching modes. [c] Symmetry and IR intensities are given in parentheses. [d] Energy of the first overtone is given in parentheses.

stretching vibrational frequencies of the free water molecule,[31] respectively, reflecting a softening of these modes upon complexation as bonding electron density is withdrawn from the water molecule.[21,32] Moreover, they lie close in energy to the $\nu_S$ and $\nu_A$ stretching vibrations observed in $[Mg(H_2O)Ar]^+$ at 3579 and 3650 cm$^{-1}$,[21,22] respectively, and we thus assign them accordingly, suggesting that water molecules bind to the Mg ion rather than to the nitrate. In the latter situation, the water molecule is expected to form symmetrical hydrogen bonds with the nitrate O-atoms, leading to considerably more red-shifted bands, as observed, for example, for $SO_2^-\cdot H_2O$ complexes (<3520 cm$^{-1}$).[33]

To test the reliability of the IRMPD spectrum, we measured the IRPD spectrum of the $[MgNO_3(H_2O)He]^+$ complex under single-photon absorption conditions (see spectrum labeled "He" in Figure 2), i.e., without the multipass cell and a nonfocused laser beam. The spectrum of the He complex shows only two bands, at 3653 and 3596 cm$^{-1}$. These are less red-shifted compared to the corresponding IRMPD bands, suggesting that the He-atom binds directly to the Mg dication and not to one

(31) Herzberg, G. *Infrared and Raman Spectra of Polyatomic Molecules*; Molecular Spectra and Molecular Structure *II*; Van Nostrand and Co., Inc.: Princeton, NJ, 1945.

(32) Vaden, T. D.; Weinheimer, C. J.; Lisy, J. M. *J. Chem. Phys.* **2004**, *121*, 3102.

(33) Woronowicz, E. A.; Robertson, W. H.; Weddle, G. H.; Johnson, M. A.; Myshakin, E. M.; Jordan, K. D. *J. Phys. Chem. A* **2002**, *106*, 7086.

of the ligands.[21] The IRMPD band labeled with an asterisk in Figure 2 is not observed in the spectrum of the He complex, which was measured at considerably lower laser fluence. It thus may be due to a transition involving a vibrational combination state, which borrows intensity from the nearby fundamental transition (see Analysis and Discussion).

Three bands of similar widths are observed in the IRMPD spectra of the $n = 2$ complex, at 3608, 3665, and 3685 $cm^{-1}$, respectively. The first and third bands show a nearly linear dependence on pulse energy, suggesting excitation of two types of fundamental ($v = 1 \leftarrow v = 0$) transitions. These two features are reminiscent of those observed for $n = 1$, and consequently they are assigned to the $\nu_S$ (3608 $cm^{-1}$) and $\nu_A$ (3685 $cm^{-1}$) stretching vibrations of the water molecules. The absence of any detectable splitting of each pair of modes, respectively, then suggests that the water molecules occupy similar binding sites around the Mg dication. The red-shift of these two bands with respect to the absorption of the free water molecules is 28% ($\nu_S$) and 40% ($\nu_A$) smaller than observed for $n = 1$, indicating that addition of a second water molecule leads to a reduction of the average ion−water molecule interaction. The intensity of the intermediate band at 3665 $cm^{-1}$ (labeled with an asterisk in Figure 2) is considerably more sensitive to the laser pulse energy: it exhibits a nonlinear, nearly quadratic behavior. By analogy to the $n = 1$ spectrum, we tentatively assign it to a combination band.

The $n = 3$ IRMPD spectrum looks quite similar to the $n = 2$ spectrum, and the band intensities exhibit the same dependence on pulse energy as discussed above. We consequently assign the 3710 $cm^{-1}$ band to the $\nu_A$ modes and the 3614 $cm^{-1}$ band to the $\nu_S$ modes of the water molecules. The absence of any detectable splitting within each group of modes, as well as the continued reduction of the red-shift of these bands (compared to the absorptions of free water), supports the picture that also the third water molecule binds directly to the Mg ion, with all three water molecules occupying similar binding sites. The additional 3692 $cm^{-1}$ band appears 27 $cm^{-1}$ higher in energy compared to that for $n = 2$, but it is at nearly the same relative position with regard to the $\nu_A$ band (−18 $cm^{-1}$).

The IRMPD spectrum for $n = 4$ shows two groups of bands, each composed of (at least) three vibrational transitions at 3620, 3630, and 3646 $cm^{-1}$ and 3706, 3717, and 3724 $cm^{-1}$, respectively. In line with the aforementioned assignments, these two groups are attributed to the $\nu_S$ and $\nu_A$ modes of the water molecules, respectively. The splitting into three components shows that the four water molecules occupy at least three different binding sites. The absence of any additional features, particularly at lower energies, suggests that all four water molecules are bound directly to the Mg ion and do not form any intermolecular water−water hydrogen bonds. Compared to the position of the corresponding bands in the $n < 4$ spectra, the center of each of the two groups continues to shift toward higher energies, i.e., toward the absorptions of the free water molecule.

The stability of the $n = 4$ complex is characterized by measuring IR spectra at elevated ion trap temperatures up to 294 K (see Figure 3). With increasing temperature, the vibrational features are expected to broaden due to population of higher rotational levels and excitation of low-frequency vibrational modes. This is what is observed, emphasizing the advantage of measuring IR spectra of internally cold ions for their structural characterization. At 100 K, most of the characteristic features in the experimental spectrum have been washed out and continue to broaden up to room temperature but without any dramatic shift or unexpected change in contour of the absorption features.

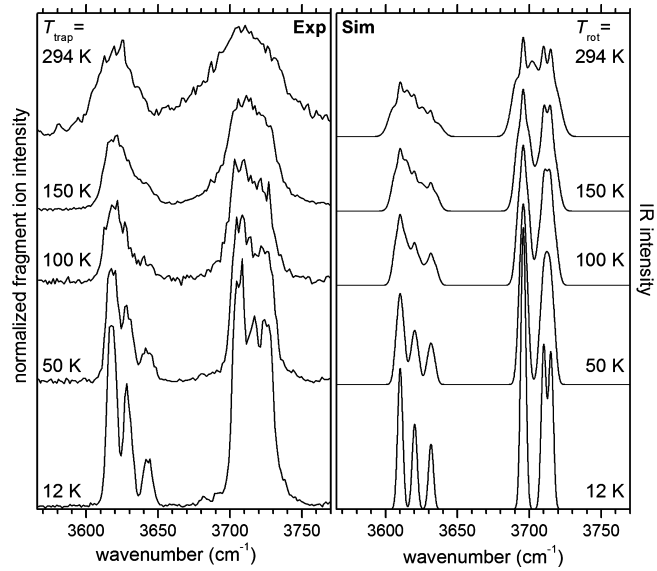


***Figure 3.*** Experimental IRMPD spectra (left) of $[MgNO_3(H_2O)_4]^+$ measured at ion trap temperatures of 12, 50, 100, 150, and 294 K. The simulated rovibrational IR spectra (right) are derived from the harmonic frequencies and equilibrium rotational constants and assuming a Boltzmann distribution for the rotational temperature. Population of low-lying excited vibrational states and other effects are neglected ($T_{vib} = 0$ K).

The following picture regarding the microhydration of $MgNO_3^+$ evolves from the above results. The first four water molecules add to the first coordination shell in $MgNO_3^+$, binding to the Mg cation and leaving the $(Mg-NO_3)^+$ ionic bond intact. For $n = 2$ and $n = 3$, the water molecule binding sites are similar, whereas for $n = 4$, the binding sites are significantly different, leading to a substantial splitting of the $\nu_S$ and $\nu_A$ modes. Assuming that nitrate binds in a bidentate fashion,[15,16] occupying two binding sites, $Mg^{2+}$ is six-fold coordinated at $n = 4$. Such a fully coordinated structure should be particularly stable, explaining its temperature stability and also the intensity pattern observed in the CID spectrum of $[MgNO_3(H_2O)_5]^+$ ions.[16] No evidence for water−water hydrogen bonds is found.

## 4. Computational Details

Density functional theory (DFT) calculations are used to identify the lowest-energy structures using the Gaussian 03 program suite.[34] The B3LYP exchange correlation functional in combination with the 6-311+G(d,p) basis set is employed. Tight convergence of the optimization and the self-consistent field procedures is imposed, and an ultrafine grid is used. Relative and dissociation energies include zero-point vibrational energies and are corrected for the basis set superposition error (BSSE). Harmonic and anharmonic vibrational frequencies are calculated with analytical second derivatives. Simulated linear absorption spectra are derived from B3LYP/6-311+G(d,p) harmonic vibrational frequencies and intensities. The harmonic frequencies are scaled by 0.956 in order to account for anharmonicities and for the method-dependent systematic errors on the calculated harmonic force constants. This scaling factor provides good agreement with the IRMPD spectra and lies in the middle of the range of scaling factors (0.950−0.963) used in comparable studies.[17,18] The resulting stick spectra are convoluted

(34) Frisch, M. J., et al. *Gaussian 03, Revision C.02*; Gaussian, Inc.: Wallingford, CT, 2004.

***Table 2.*** B3LYP/6-311+G(d,p) Relative Energies $E$ (kJ/mol), Lowest Dissociation Energies $E_{diss}$ (kJ/mol), and Characteristic Bond Lengths (Å) of Bare and Microhydrated $[MgNO_3(H_2O)_n]^+$ Complexes ($n = 0-4$)

| $n$ | isomer | state | $E$ | $r_{Mg-N}$ | $r_{Mg-OH_2}$ | $E_{diss}$ |
|---|---|---|---|---|---|---|
| 0 | 00-Bi | $^1A_1$ ($C_{2v}$) | 0.0 | 2.36 | | 1395.9 ($NO_3^-$-loss) |
| 1 | 10-Bi | $^1A_1$ ($C_{2v}$) | 0.0 | 2.38 | 1.99 | 208.3 ($H_2O$-loss) |
| 2 | 20-Bi | $^1A$ ($C_2$) | 0.0 | 2.41 | 2.02, 2.02 | 152.2 ($H_2O$-loss) |
| | 11-Bi | $^1A'$ ($C_s$) | 63.7 | 2.39 | 1.95, 3.93 | |
| 3 | 30-Bi | $^1A'$ ($C_s$) | 0.0 | 2.46 | 2.05, 2.05, 2.06 | 114.2 ($H_2O$-loss) |
| | 30-Mono | $^1A$ ($C_1$) | 37.6 | 2.93 | 1.97, 2.03, 2.04 | |
| | 21-Bi-I | $^1A$ ($C_1$) | 39.3 | 2.42 | 1.97, 2.03, 3.98 | |
| | 21-Bi-II | $^1A_1$ ($C_{2v}$) | 40.7 | 2.41 | 2.01, 2.01, 3.75 | |
| 4 | 40-Bi | $^1A'$ ($C_s$) | 0.0 | 2.49 | 2.08, 2.09, 2.14, 2.14 | 71.7 ($H_2O$-loss) |
| | 31-Bi | $^1A$ ($C_1$) | 5.6 | 2.49 | 2.00, 2.06, 2.07, 3.63 | |
| | 40-Mono | $^1A'$ ($C_s$) | 16.9 | 3.03 | 2.02, 2.07, 2.07, 2.10 | |
| | 31-Mono | $^1A'$ ($C_s$) | 41.7 | 2.96 | 1.97, 2.03, 2.03, 3.79 | |
| 1·He | 10-Bi | $^1A'$ ($C_s$) | 0.0 | 2.38 | 2.00 | 1.9 (He-loss) |

using a Gaussian line shape function with a width of 6 $cm^{-1}$ (fwhm) to account for the laser bandwidth, as well as broadening due to rotational excitation. Further computation with the Turbomole V6.0 program package[35−38] at the B3LYP/def2-TZVP theory level yields results consistent with the Gaussian 03 calculations (see Table S1 in the Supporting Information).

## 5. Analysis and Discussion

**Minimum Energy Structures.** The B3LYP/6-311G+(d,p) minimum energy structures of $[MgNO_3(H_2O)_n]^+$ with $n = 1-4$ are shown in Figure 4, and selected properties are listed in Table 2. We find structures similar to those reported previously using the MP2/aug-cc-pVDZ level of theory.[16] The nitrate ion binds in a bidentate fashion to the Mg ion, and the first four water molecules then fill the first coordination shell of the dication. The first water molecule binds opposite to and in the plane spawned by the nitrate ion, resulting in a $C_{2v}$ structure, labeled 10-Bi in Figure 4, with a $Mg^{2+}$−water distance $r_{Mg-OH_2}$ of 1.99 Å. [Note on the nomenclature: Using *ij*-Bi or *ij*-Mono, *i* denotes the number of water molecules in the first coordination shell, and *j* denotes the number of water molecules in the second coordination shell. The number of coordination sites the nitrate ion occupies is either one (Mono) or two (Bi).] Addition of a second water molecule yields the $C_2$ structure 20-Bi, in which the two water molecules are symmetry-equivalent ($r_{Mg-OH_2}$ = 2.02 Å), and both form a weak H-bond (3.28 Å) to one of the nitrate O-atoms. For $n = 3$, a $C_s$ structure (30-Bi) is found to be lowest in energy. The in-plane water molecule ($r_{Mg-OH_2}$ = 2.06 Å) forms a H-bond with one of the O-atoms of the nitrate, while the other two (out-of-plane) water molecules ($r_{Mg-OH_2}$ = 2.05 Å) occupy symmetry-equivalent binding sites, and each forms an H-bond with another O-atom. The $n = 4$ complex exhibits a quasi-octahedral structure (40-Bi), with the two symmetry-equivalent water molecules being slightly farther away ($r_{Mg-OH_2}$ = 2.14 Å) from the $Mg^{2+}$ ion than the two with O-atoms in the symmetry plane (2.08 and 2.09 Å). Summarizing, the Mg−water distance increases monotonically from 1.99 Å in $n = 1$ to up to 2.14 Å in $n = 4$, and only for $n = 4$ do these distances differ substantially between binding sites.

Most other structural isomers are found significantly higher in energy (see Figure 4). No minimum was found for a water molecule binding exclusively to the nitrate ion. Starting with $n = 2$, isomers with one water in the second coordination shell are found. They lie 63.7 (11-Bi), 39.3 (21-Bi-I), 40.7 (21-Bi-II), 5.6 (31-Bi), and 41.7 kJ/mol (31-Mono) higher in energy. At least three water molecules are needed to stabilize the nitrate ion in a monodentate configuration. These isomers are found 37.6 (30-Mono) and 16.9 kJ/mol (40-Mono) above the respective global minimum energy structure.

**Dissociation Energies and Absorption Mechanism.** The calculated, BSSE-corrected dissociation energies for the loss of one water molecule for the $n = 1-4$ complexes are 208.3, 152.2, 114.2, and 71.7 kJ/mol (see Table 2), respectively. Thus, for all complexes the absorption of more than a single IR photon is required to overcome the dissociation limit. Assuming internally cold complexes, the absorption of at least two ($n$ = 4), three ($n = 3$), four ($n = 2$), or five photons ($n = 1$) is required at 3700 $cm^{-1}$.

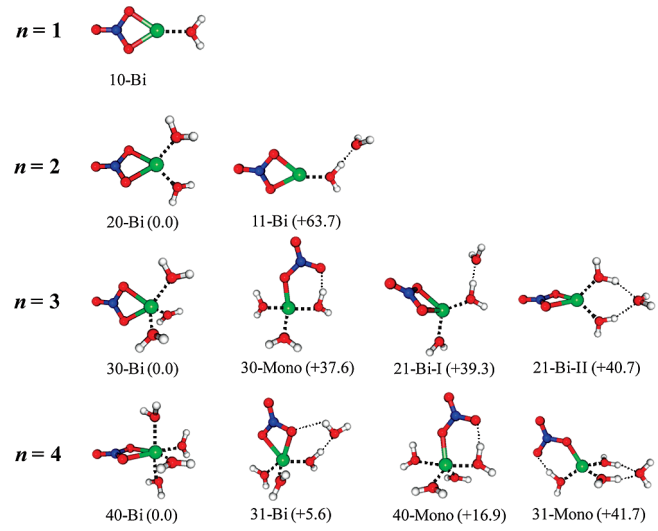


***Figure 4.*** B3LYP/6-311+G(d,p) minimum-energy structures of the $[MgNO_3(H_2O)_n]^+$ complexes.

(35) Ahlrichs, R.; Bär, M.; Häser, M.; Horn, H.; Kölmel, C. *Chem. Phys. Lett.* **1989**, *162*, 165.
(36) Treutler, O.; Ahlrichs, R. *J. Chem. Phys.* **1995**, *102*, 346.
(37) Eichkorn, K.; Treutler, O.; Öhm, H.; Häser, M.; Ahlrichs, R. *Chem. Phys. Lett.* **1995**, *242*, 652.
(38) *TURBOMOLE V6.0*; University of Karlsruhe and Forschungszentrum Karlsruhe GmbH, 1989−2007, TURBOMOLE GmbH (since 2007), 2009; http://www.turbomole.com.

An efficient multiple-photon absorption mechanism involves fast internal vibrational energy redistribution (IVR).[39] Assuming an IVR lifetime ($\tau_{IVR}$) of <1 ns, the criterion of stochasticity,[40]

$$\hbar/\tau_{IVR} > \sigma^{-1}$$

where $\hbar$ is Planck's constant divided by $2\pi$, yields a lower limit for the density of states of $2 \times 10^2$ states/cm$^{-1}$. The vibrational density of states at 3700 cm$^{-1}$ for the $n = 1$ complex, estimated using the Beyer−Swinehart algorithm,[41] is $2 \times 10^4$ states/cm$^{-1}$, 2 orders of magnitude above this limit, suggesting that noncoherent absorption of multiple photons should be efficient at sufficiently high photon fluence. In this case, the IRMPD spectra can be qualitatively interpreted in terms of linear absorption spectra, because the resonant absorption of the first photon is the "rate"-determining process. Coherent multiphoton absorption processes, on the other hand, are improbable under the present experimental conditions (laser pulse intensity <1 GW/cm$^{-2}$).

**Harmonic Spectra.** Simulated linear absorption spectra, derived from scaled harmonic vibrational frequencies of the structures shown in Figure 4 (see also Table S2 of the Supporting Information), are compared to the experimental IRMPD spectra in Figure 2. Satisfactory agreement with the experimental data, in particular with the relative band positions of the fundamental transitions and the size-dependent trends, is observed, supporting our initial assignment of these bands. Moreover, the simulated spectra of the energetically higher-lying isomers, namely those with a water molecule in the second coordination shell or with nitrate in monodentate coordination, do not agree with the experimental data, excluding them from the assignment. For $n = 4$, for example, the 31-Bi isomer is calculated only 5.6 kJ/mol higher in energy than the 40-Bi isomer. A closer look at Figure 2 and Table S2 reveals, however, that only the latter reproduces the measured IR spectrum satisfactorily, in particular with respect to the position and relative intensity of the lowest-energy $\nu_S$ mode (3591 cm$^{-1}$). Even at higher temperatures (see Figure 3), little dissociation signal is observed below 3600 cm$^{-1}$, suggesting that the 31-Bi isomer is not significantly populated up to 294 K.

The measured (calculated) ratios of intensities between the $\nu_A$ and $\nu_S$ modes, $I(\nu_A)/I(\nu_S)$, for $n = 1-4$ are 0.8 (1.5) 1.0 (1.7), 1.2 (1.8), and 2.3 (2.1), respectively, significantly smaller than the calculated ratio of 18 for the free water molecule.[42] The enhancement of the $\nu_S$ relative to the $\nu_A$ mode upon complexation results from the electrostatic interaction between the ion and the water dipole moment.[32] It decreases monotonically with increasing cluster size as the average water−ion interaction strength decreases. Interestingly, the measured ratios are noticeably smaller than the calculated ones for $n = 1-3$. Lower intensities upon excitation of the water $\nu_A$ mode compared to excitation of the $\nu_S$ mode observed in the IRMPD spectra vs those predicted for linear absorption spectra have been previously reported, for example for $NH_4^+(H_2O)$,[43] and rationalized by considering the different time scales for IVR, resulting from excitation of the molecules parallel ($\nu_S$) and perpendicular ($\nu_A$) to the hydrogen bond, through which IVR needs to proceed.

Finally, for $n = 1$, the $\nu_A$ band appears broader than the $\nu_S$ band in both of the spectra shown in Figure 2. This results from the different selection rules that apply to excitation of the water symmetric and antisymmetric stretching vibrations in $n = 1$. Assuming a quasi-symmetric top, the symmetric stretching transitions are parallel transitions with $\Delta K = 0$, while the antisymmetric stretching transitions are perpendicular transitions with $\Delta K = \pm 1$. Consequently, the three peaks observed in the IRMPD spectrum between 3615 and 3665 cm$^{-1}$ may be tentatively attributed to the P, Q, and R branches of this perpendicular transition, suggesting that, for $n = 1$, rotationally hotter ions are more efficiently photodissociated.

**Anharmonic Calculations.** To understand some remaining discrepancies between the harmonic and the experimental IR spectra, we performed anharmonic calculations. Inclusion of anharmonicity leads to a reduction of the harmonic vibration frequencies of the fundamental transitions by 5%, overshooting the experimental band positions by roughly 1%. Agreement with regard to the relative band positions is slightly improved compared to that found for the harmonic spectra. Interestingly, the first overtones of the $\nu_A$ modes for $n = 2$ and 3 (see Table 1) are in excellent agreement with twice the value of the bands labeled with asterisks in the experimental spectra, observed 20 ($n = 2$) and 18 cm$^{-1}$ ($n = 3$) below the $\nu_A$ band. This suggests that the $\nu_A$ overtone states may be involved in the sequential multiple-photon absorption process. In more detail, the asterisk-labeled bands could theoretically be due to a coherent two-photon absorption process, but this is highly unlikely at the low laser fluences used in the present experiment. Excitation of a "dark" combination state $\nu_c$, which borrows some intensity from the nearby, "bright" fundamental transition $0 \rightarrow \nu_A$, followed by absorption of a second photon, leading to excitation of the "bright" overtone states ($2\nu_A$) before vibrational energy redistribution occurs, is more probable. The $0 \rightarrow \nu_c \rightarrow 2\nu_A$ absorption process would account for both the observation of the asterisk-labeled bands in our spectra and the different dependence of their intensity on laser energy compared to the excitation of the "bright" fundamental states. Based on the calculated vibrational frequencies, $\nu_c = \nu_S + \nu_{LIB}$ is the only reasonable candidate, where $\nu_{LIB}$ denotes one of the two lowest-frequency water librational modes (~50 cm$^{-1}$). A similar argument holds for the $n = 1$ spectrum. In this case, the $2\nu_S$ overtone state is involved in the excitation process, leading to the appearance of the asterisk-labeled band; however, the nature of the combination state is less clear. For $n = 4$, on the other hand, these bands are not observed, because those spectra were measured at a lower laser pulse energy than was used for the measurement of the $n = 1-3$ spectra.

**Rotational Band Profiles.** Simulated rotational band profiles can be used to qualitatively understand the IRMPD spectra measured at elevated temperatures (see Figure 3). Note that this is only a very crude simulation, as important effects like the thermal population of low-lying vibrationally excited states, as well as freely rotating water molecules, which may lead to additional features, are completely neglected. Nonetheless, our crude simulations do reproduce the changes upon heating of the clusters qualitatively, in particular for the $\nu_S$ band, suggesting that an increase in internal energy of the $n = 4$ complex does not induce isomerization; that is to say, the $n = 4$ cluster is stable also at room temperature.

(39) Mukamel, S.; Jortner, J. *J. Chem. Phys.* **1976**, *65*, 5204.
(40) Bagratashvili, V. N.; Letokhov, V. S.; Makarov, A. A.; Ryabov, E. A., *Multiple Photon Infrared Laser Photophysics and Photochemistry*; Harwood Academic Publishers GmbH: Amsterdam, 1985.
(41) Beyer, T.; Swinehart, D. F. *Commun. ACM* **1973**, *16*, 379.
(42) Galabov, B.; Yamaguchi, Y.; Remington, R. B.; Schaefer, H. F. *J. Phys. Chem. A* **2002**, *106*, 819.
(43) Pankewitz, T.; Lagutschenkov, A.; Niedner-Schatteburg, G.; Xantheas, S. S.; Lee, Y. T. *J. Chem. Phys.* **2007**, 126.

## 6. Summary and Conclusions

In this study, a Herriott-type multipass cell was used to measure gas-phase vibrational spectra of $[MgNO_3(H_2O)_{1-4}]^+$ in the O−H stretching region by IRMPD spectroscopy. The combination of experimental and simulated harmonic and anharmonic IR spectra allows for an unambiguous identification of the lowest-energy structures of microhydrated $[MgNO_3(H_2O)_{1-4}]^+$ complexes. Temperature-dependent IRMPD spectra of $[MgNO_3(H_2O)_4]^+$ in the range from 12 to 294 K reveal that the $n = 4$ cluster is very stable, even at room temperature. The present results show that the first four water molecules only weakly perturb the ionic bond in this prototypical salt, and many more water molecules are needed to form a solvent-separated ion pair. However, the techniques described here can readily be extended to the study of the structure and stability of larger complexes ($n > 4$), and it will be interesting to see in what size and temperature regime the bulk-like behavior will be approached.

**Acknowledgment.** L.J. thanks the Alexander von Humboldt Foundation for a postdoctoral scholarship. We thank Boris G. Sartakov for helpful discussions.

**Supporting Information Available:** Complete ref 34; Table S1, comparison of B3LYP/6-311+G(d,p) and B3LYP/def2-TZVP energies; Table S2, calculated and scaled (0.956) O−H stretching vibrational frequencies of several low-lying isomers at the B3LYP/6-311+G(d,p) level of theory; Cartesian coordinates for all isomers shown in Figure 4. This material is available free of charge via the Internet at http://pubs.acs.org.

JA1011806